

PCCP

Accepted Manuscript



This is an *Accepted Manuscript*, which has been through the Royal Society of Chemistry peer review process and has been accepted for publication.

Accepted Manuscripts are published online shortly after acceptance, before technical editing, formatting and proof reading. Using this free service, authors can make their results available to the community, in citable form, before we publish the edited article. We will replace this *Accepted Manuscript* with the edited and formatted *Advance Article* as soon as it is available.

You can find more information about *Accepted Manuscripts* in the [Information for Authors](#).

Please note that technical editing may introduce minor changes to the text and/or graphics, which may alter content. The journal's standard [Terms & Conditions](#) and the [Ethical guidelines](#) still apply. In no event shall the Royal Society of Chemistry be held responsible for any errors or omissions in this *Accepted Manuscript* or any consequences arising from the use of any information it contains.

Enhanced performance and Morphological Evolution of PTB7:PC₇₁BM Polymer Solar Cells by Using Solvent Mixtures with Different Additives

Di Huang^{a,b} Yang Li^{a,b} Zheng Xu^{a,b,*} Suling Zhao^{a,b} Ling Zhao^{a,b} Jiao Zhao^{a,b}

a. Key Laboratory of Luminescence and Optical Information, Beijing Jiaotong University, Ministry of Education, Beijing 100044, PR China

b. Institute of Optoelectronic Technology, Beijing Jiaotong University, Beijing 100044, PR China

Abstracts

Organic photovoltaics (OPVs) were fabricated with blended active layers of poly[[4,8-bis[(2-ethylhexyl)oxy]benzo[1,2-b:4,5-b']dithiophene-2,6-diyl][3-fluoro-2-(2-ethylhexyl)carbonyl]thieno[3,4-b]thiophenediyl]: [6,6]-phenylC₇₁-butyric acid methyl ester (PTB7:PC₇₁BM). The active layers were prepared in chlorobenzene (CB) with different additives of 1,8-Diiodooctane (DIO) and 1,8-Dibromooctane and different concentrations by a wet process with spin coating. The effects of different solvent additives were studied with respect of photovoltaic parameters such as fill factor, short circuit current density, and power conversion efficiency. The absorption and surface morphology of the active layers were investigated by UV-visible spectroscopy, atomic force microscopy (AFM) and time-of-flight secondary ion mass spectrometer (TOF-SIMS), respectively. The results indicated that structural and morphological changes were induced by the solvent additives. The polymer solar cells (PSCs) of PTB7/PC₇₁BM prepared with DIO and 1,8-Dibromooctane showed more improved PCE of 6.76% by spin coating method. The enhancement of performance of PSCs could be mainly attributed to the absorption enhancement and the improved charge carrier transportation.

*Corresponding authors: Tel.: +86 010 51684858.
E-mail addresses: zhengxu@bjtu.edu.cn (Z.Xu).

1. Introduction

Organic photovoltaics (OPVs) have developed rapidly over the last decade because of their high possibility of commercialization based on solution process.¹⁻³ Recent progress in organic solar cell development have demonstrated an impressive improvement in the power conversion efficiency (PCE) which have already reached 9.35%.⁴

Poly[[4,8-bis[(2-ethylhexyl)oxy]-benzo[1,2-b:4,5-b0]dithiophene-2,6-diyl][3-fluoro-2-[(2-ethylhexyl)carbonyl]thieno[3,4-b]thiophenediyl]] (PTB7) is a promising electron donor material, which could be blended with [6,6]-phenyl-C₇₁-butyric acid methyl ester (PC₇₁BM) as an electron acceptor material and yield a power conversion efficiency (PCE) over 8% in a single bulk hetero-junction device structure.⁵ Due to its low-band-gap, PTB7 can efficiently absorb photons at long wavelengths. However, in order to be commercially comparable with other types of photovoltaic devices, further effort is still required to further improve the PCEs of OPVs.^{6,7}

Several approaches have been addressed as the efforts to further improve the PCE of polymer bulk heterojunction (BHJ) solar cells which includes synthesizing new active materials, varying the donor-acceptor ratio, using solvent additives⁸⁻¹⁰ and so on. Among them, solvent additives have been widely adopted because of their simpler inclusion in experimental operations as compared with conventional thermal annealing processes and ideal bulk heterojunction may be achieved in an active layer.¹¹ 1,8-Diiodooctane (DIO) is one of the most popular solvent additives that have been used to improve the morphology of the active layer of BHJ solar cells, especially for OPVs with low-band-gap polymers such as poly[2,1,3-benzothiadiazole-4,7-diyl[4,4-bis(2-ethylhexyl)-4H-cyclopenta[2,1-b:3,4-b']dithiophene-2,6-diyl]] (PCPDTBT) and Poly[N-9'-heptadecanyl-2,7-carbazole-alt-5,5-(4',7'-di-2-thienyl-2',1',3'-benzothiadiazole)](PCDTBT)^{8,12}. On the other hand, 1,8-Dibromooctane, 1,8-Dioctanedithiol, and 1,8-Octanedithiol are also used as solvent additives to improve PCE of BHJ solar cells.¹²

In this letter, 1,8-Dibromooctane was used as the solvent additive to fabricate BHJ polymer solar cell based on PTB7/PC₇₁BM as the active layer. DIO and/or 1,8-Dibromooctane were varied with different ratios during the solution preparation of the organic active layer. The effect of the solvent additives was investigated in PTB7:PC₇₁BM blended films. The morphology of the active layer with different solvent additive ratios has been studied and the related OPV device performance also has been reported.

For the convenience of discussion, different films and devices were named and prepared to compare their performances:

Film 1: PTB7:PC₇₁BM,

Film 2: PTB7:PC₇₁BM, 3 v/v % 1,8-Dibromooctane

Film 3: PTB7:PC₇₁BM, 3 v/v % DIO

Film 4: PTB7:PC₇₁BM, 3 v/v % 1,8-Dibromooctane and 3 v/v % DIO

Device 1: ITO/PEDOT:PSS /film1/LiF/Al

Device 2: ITO/PEDOT:PSS /film2/ LiF/Al

Device 3: ITO/PEDOT:PSS /film3/ LiF/Al

Device 4: ITO/PEDOT:PSS /film4/ LiF/Al

2. Experimental Section

2.1. Fabrication of solar cells

PC₇₁BM, and 1,8-Dibromooctane were purchased from, Nano-C, and Sigma-Aldrich respectively. PTB7 was supplied by 1-Material with a molecular weight of ~200 kg/mol and polydispersity of ~4. PTB7 and PC₇₁BM were co-dissolved in chlorobenzene at 20 mg/ml with a weight ratio of 1: 1.5 to form a mixed solution. Moreover, organic materials were weighed and dissolved in ambient air conditions. The devices were fabricated with an architecture of ITO/poly(3,4-ethylenedioxythiophene):poly(styrenesulfonate)/PTB7:PC₇₁BM/LiF /Al. The indium tin oxide (ITO) glass substrates with sheet resistance of 10 Ω/□ were cleaned

consecutively in ultrasonic bathes containing glass lotion, ethanol and de-ionized water and then dried by high pure nitrogen gas. The pre-cleaned ITO substrates were then treated by UV-ozone for 5 min for further cleaning the substrates and improving the work function of ITO substrates. The PEDOT:PSS (purchased from Clevios AI 4083.) was spin-coated on the ITO substrates at 3000 rounds per minute (rpm) for 50s. Then PEDOT: PSS coated ITO substrates were dried in air at 150 °C for 20 min. The substrates were then transferred to a nitrogen-filled glove box. On the other hand, in order to fabricate the different devices as designed in experiment, 1%, 3% and 5% of 1,8-Dibromooctane by volume were added into PTB7/PC₇₁BM mixed solution, respectively. The active layers with different ratios of 1,8-Dibromooctane were then formed by spin-coating on the PEDOT:PSS with same spin-coating parameters: 1s for acceleration and 120s with a rotation speed of 1000 rpm. On the top of the active layer, a 0.8 nm interfacial layer LiF was deposited under 4×10^{-4} Pa vacuum conditions. The thickness of LiF was monitored by a quartz crystal microbalance. An aluminum cathode layer of about 100 nm was then deposited on LiF layer under 10^{-4} Pa vacuum conditions. The active area was defined by the vertical overlap of ITO anode and Al cathode which is about 9 mm².

2.2. Photovoltaic characterization

The absorption spectra of films were measured with a Shimadzu UV-3101 PC spectrometer. The film thickness were measured by the KLA Tencor P6 stylus profiler. The thickness of film 1, film 2, film 3 and film 4 were 89nm, 83nm, 71nm and 59nm respectively. The current–voltage (J-V) characteristics and capacitance–voltage (C-V) characteristics of PSCs were measured by using a Keithley 4200 semiconductor characterization system under a simulated AM 1.5G spectrum with the power of 100 mW/cm² generated by ABET Sun 2000 solar simulator. C-V measurements were carried out in the dark. For C-V measurements, the dc bias

voltage sweep (-2 V to 1.5 V) was superimposed by a low frequency (2 kHz) ac voltage with a small amplitude (100 mV) to prevent any influence of the ac signal on the measured capacitance. The corresponding J–V curves were recorded from -1 V to 1 V with an interval of 0.01 V . An incident photon to current conversion efficiency (IPCE) spectrum was measured on Zolix Solar Cell Scan 100. The morphology of the films was investigated by atomic force microscopy (AFM) using a multimode Nanoscope IIIa operated in tapping mode. All the samples were measured with scan sizes of $5 \times 5\ \mu\text{m}^2$. Secondary ion mass spectrum was obtained by using a time-of-flight secondary ion mass spectrometer TOF-SIMS 5 from ION-TOF GmbH (Munster, Germany). A Bi_1^+ liquid metal ion gun operating at a 30keV beam voltage with a 45° incident angle was used. The depth profiling experiment was performed using a gas cluster ion gun Ar_{1700}^+ with an analyzed area of $100 \times 100\ \mu\text{m}$ inside an etching area of $500 \times 500\ \mu\text{m}$. All analyses were carried out at 256×256 pixels. Charge compensation with an electron flood gun was used during the analysis cycles. Negative ion mode spectra were calibrated on the C^- , CH^- , C_2^- and C_2H^- peaks. Moreover all the tests were in ambient air conditions.

3. Results and discussion

The J – V characteristic curves of PSCs with different 1,8-Dibromooctane ratios are shown in **Fig. 1a**. The PV performances of PSCs were summarized according to J–V curves and are listed in **Table 1**. Among all the different ratios, it can be found that the device with 3 v/v % of 1,8-Dibromooctane demonstrated the highest median PCE of 4.70% along with a short-circuit current J_{sc} of 11.11 mA/cm^2 , an open-circuit voltage V_{oc} of 0.75 V , and a FF of 56.50%. This PCE was 71.5% higher than that of the control device which was 2.74%. The data in Table 1 shows that the PCE

improvement was mainly attributed to the enhancement in the J_{sc} and FF, where J_{sc} increased from 7.22 mA/cm^2 to 11.11 mA/cm^2 with 53.9% increasing while FF increased from 49.98% to 56.50% with 13.0% increasing, respectively. To further investigate the mechanism responsible for the enhanced performance of the PSCs with 1,8-Dibromooctane additive, the optimized volume ratio of 3% was used.

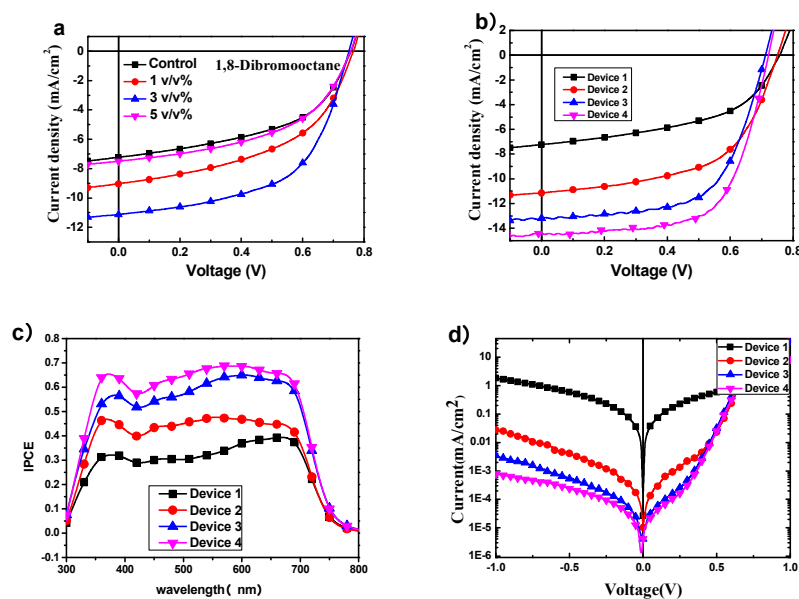


Fig. 1. (a) The J–V characteristic curves of solar cells with different doping ratio of 1,8-Dibromooctane under AM 1.5 light power of 100 mW/cm^2 ; (b) The J–V characteristic curves of solar cells without or with 3 v/v % DIO and/or 3 v/v % 1,8-Dibromooctane; (c) Incident photon to collected electron (IPCE) of the devices in the system of PTB7:PC71BM without or with 3 v/v % DIO and/or 3 v/v % 1,8-Dibromooctane; (d) J–V characteristics cast from solar cells without or with 3 v/v % DIO and/or 3 v/v % 1,8-Dibromooctane in darkness.

Table 1: The PV performance of ITO/PEDOT:PSS/PTB7:PC₇₁BM/LiF/Al photovoltaic devices with different doping ratio of 1,8-Dibromooctane.

Doping ratio	Voc[V]	Jsc[mA/cm ²]	FF[%]	PCE[%]
Control	0.75	7.22	49.98	2.74
1 v/v %	0.76	9.04	49.54	3.41
3 v/v %	0.75	11.11	56.50	4.70
5 v/v %	0.76	7.49	49.59	2.82

The J–V curves of PSCs with different solvent additives under illumination of

simulated AM1.5G (100 mW/cm²) are shown in **Fig. 1b** and **Table 2** summarizes the device performance results. Device 1 demonstrated a PCE of 2.74% with a J_{sc} of 7.22 mA / cm², an V_{oc} of 0.74 V, and a FF of 50.0%. As shown in **Table 2**, with the addition of 3 vol % 1,8-Dibromooctane (volume fraction of chlorobenzene) in Device 2, J_{sc} increased to 11.11mA/cm² and FF increased to 56.50%, which resulted in a PCE of 4.70%. If both 3.0 v/v % DIO and 3.0 v/v% 1,8-Dibromooctane were added to the solution prior to spin casting, PCE of device 4 was further increased to 6.76% along with a V_{oc} of 0.72 V, a J_{sc} of 14.35 mA/cm², and a FF of 65.4%. The improved J_{sc} value was confirmed by measuring the incident photon to converted electron ratios (IPCE) (Fig. 1c). The maximum IPCE value of the PSCs without additive was 39.4%, and it was increased to 68.8% for PSCs with 3 v/v% DIO and 3 v/v % 1,8-Dibromooctane. Note that theoretical J_{sc} obtained by integrating the product of the IPCE data in Fig. 1c and the AM 1.5G solar spectrum (7.65 mA cm⁻² and 14.63 mA cm⁻² for the devices without additive and with 3 v/v% DIO and 3 v/v % 1,8-Dibromooctane respectively), which are in good agreement with the values obtained from the J–V characteristics (Fig. 2b, Table 2).⁵ The single logarithmic dark current curves show that device 4, device 3 and device 2 have smaller leakage current compared with device 1, as shown in **Fig. 1d**. It is well-known that the leakage current is determined by the shunt resistance (R_{sh}).¹³ The larger R_{sh} indicates a lower charge carrier recombination in active layer. This indicates that DIO and/or 1,8-Dibromooctane can effectively restrain the leakage current under reverse bias, which may provide effective charge carriers transport in the blend layers, resulting in the increase in J_{sc}, compared to that of device 1. The smaller R_s indicates a lower resistance of the semiconductor bulk resistance and a better metal/semiconductor interface connection induced by using co-additives.¹³

Table 2: Summary of photovoltaic parameters of PTB7: PC₇₁BM system solar cells without or with 3 v/v % DIO and/or 3 v/v % 1,8-Dibromooctane.

	V _{oc} [V]	J _{sc} [mA/cm ²]	FF[%]	PCE[%]	R _{sh} [Ωcm ²]	R _s [Ωcm ²]
Device 1	0.75	7.22	50.0	2.74	384.6	17.6
Device 2	0.75	11.11	56.5	4.70	461.1	12.9

Device 3	0.71	13.19	61.9	5.80	738.9	6.6
Device 4	0.72	14.35	65.4	6.76	1878.9	5.2

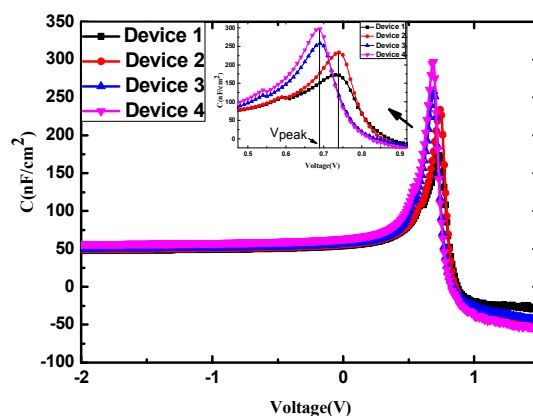


Fig. 2. Capacitance vs. voltage plot of the devices.

We also investigated the effect of PTB7: PC₇₁BM system solar cells without or with 3 v/v% DIO and/or 3 v/v % 1,8-Dibromooctane by measuring the capacitance–voltage (C–V) characteristics (**Fig.2**). The accumulated space charge inside the device can increase its capacitance. As the applied voltage increased, the capacitance tended to increase to a peak and then decrease. The V_{bi} is correlated with the voltage V_{peak} at the peak capacitance as^{14, 15}

$$V_{bi} - V_{peak} \propto \frac{k_B T}{e} \quad (1)$$

Where V_{bi} is the built-in potential in the devices, k_B is the Boltzmann constant, T is the absolute temperature, e is the magnitude of the electron charge. In photovoltaic devices, a higher V_{peak} implies a higher V_{bi} and thus higher V_{oc} .^{16, 17} The tendency of V_{peak} without or with 3 v/v % DIO and/or 3 v/v % 1,8-Dibromooctane obtained in **Fig.2** perfectly matches the V_{oc} measured from J –V characteristics.

To understand the roles of solvent additives in the mixture of PTB7 and PC₇₁BM, further characterization was carried out to study the surface morphology, optical and electrical properties of the blended films without or with 3 v/v% DIO and/or 3 v/v % 1,8-Dibromooctane. The absorption spectra of the neat PC₇₁BM and PTB7 films are shown in **Fig. 3a**. PC₇₁BM has two apparent absorption peaks at 375 nm and 480 nm, which widen the active layer absorption in the short wavelength range. The absorption

spectra of PTB7 shows an apparent complementary absorption in the range from 550 nm to 750 nm. Two broad absorption peaks at around 624 and 682 nm are attributed to the characteristic Π - Π^* transition of the PTB7 polymer.^{9, 18 19} Comparing the absorption spectra of the films prepared with and without solvent additives, there was no obvious peak shift both in the films prepared with organic additives and in the films prepared with pristine CB, as shown in **Fig. 3b**. It indicates that the thin films prepared with additives have an amorphous phase. On the other hand, it can be found there is an obvious increase of relative absorption intensity in the region of 300–800 nm for film 2, film 3 and film 4. This result indicated that the films with solvent additives can harvest solar photons more effectively than the film without solvent additives under the same conditions. The more light absorption the higher photocurrent generation.²⁰ It's the reason why the J_{sc} increased with solvent additives. On the basis of IPCE and absorption results, it is clear that DIO and 1,8-Dibromooctane as co-additives greatly broaden the wavelength range for absorption enhancement compared with either 1,8-Dibromooctane or DIO.

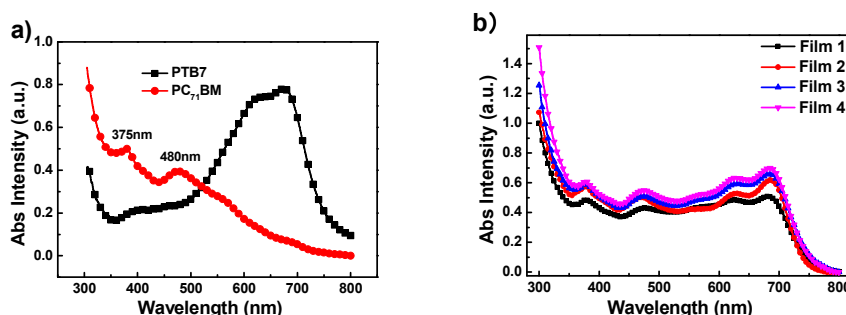


Fig. 3. (a) The absorption spectra of neat PTB7 and PC₇₁BM films; (b) absorption spectra of PTB7/PC₇₁BM films cast from solvents with or without DIO and/or 1,8-Dibromooctane additives. The data was normalized by the film thickness.

In order to investigate the effect of DIO and/or 1,8-Dibromooctane on the morphology of blend films, the surface topography and phase images of the blend films was studied by atomic force microscopy (AFM) in tapping mode ($5 \mu\text{m} \times 5 \mu\text{m}$). **Fig.4** shows atomic force microscopy (AFM) images of film 1, film 2, film 3 and film 4. It has been found that film 1 was formed by uniformly distributed grains with grain size from ≈ 50 nm to 300 nm, which are identified as large PC₇₁BM rich domains embedded in a polymer matrix, appearing as dark region in the images, agreeing with

many other researches on polymer:fullerene BHJ system.^{9, 21, 22} It can indicate that PTB7 and PC₇₁BM might not have good mutual solubility so that the fullerenes actually aggregated in certain degree.²³⁻²⁵ When 3 v/v% of 1,8-Dibromooctane was added, the number of the grains was reduced dramatically although the grain size increased to about 400nm, which implies that the mutual solubility of polymers increased with the help of 1,8-Dibromooctane, however, it was still not sufficient enough to avoid fullerenes aggregation during the film formation. A mutual interaction between the molecules might have an influence on the blend film formation.²⁶ On the other hand, film 3 reveals no obvious grain on the surface, indicating that there is sufficient mutual solubility of polymers which leads to an interpenetrated blending through excellent percolation of the polymers. The polymer chains of PTB7 and PC₇₁BM are fully extended and entangled with each other. No obvious aggregation can be observed. This will definitely prevent carriers from recombination and improve the carrier transport, which could be contributed to the distinctively enhanced PCE (5.80%) of the resulting OPV.^{9, 27} It also can be the reason why device 2 reveals a mode rate PCE of 4.46%, which is distinctively lower than that of device 3, although it is rather higher than device 1. For device 4, it can be seen that the roughness (RMS) of film 4 has been increased slightly compared to that of film 3, which implies the co-additive effect might have resulted in a moderate formation of the nano morphology of molecules, which leads to the PCE of the OPV further improved to 6.76%.²⁸

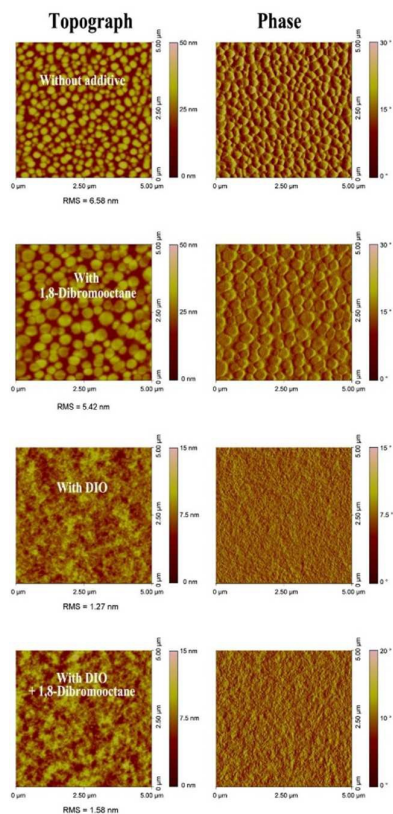


Fig. 4. The AFM surface topography and phase images of the PTB7:PC₇₁BM films with/without 3 v/v % DIO and/or 3 v/v % 1,8-Dibromooctane

The surface of the film prepared with additives appeared to be smoother than that of the film prepared without additives, which suggested a well-mixed heterojunction. We next characterized chemical compositions of the blends as a function of the sputter time, using surface mapping analysis. **Fig. 5** shows the yield of fluorine ions (F⁻) as a function of the sputter time, obtain using time-of-flight secondary ion mass spectrometer (TOF-SIMS). The F⁻ are unique to PTB7.^{29,30} The F⁻ yield of the film 1 induced a more obvious reduction than that of the film 2, film 3 and film 4 from 5s to 150s, as indicated in both **Fig. 5** and **Table 3**. The results gave evidence that the distribution of PTB7 molecules in the film with additives was more evenly distributed than that of PTB7 molecules in the film without additives in the vertical direction. Meanwhile, they also demonstrated an even distribution of PC₇₁BM. What's more, the PTB7 domains with additives were more evenly distributed along the vertical direction compared with domains of those without additives. This suggested that the chemical composition of the blend along the vertical direction changed, as illustrated

in Fig. 6.

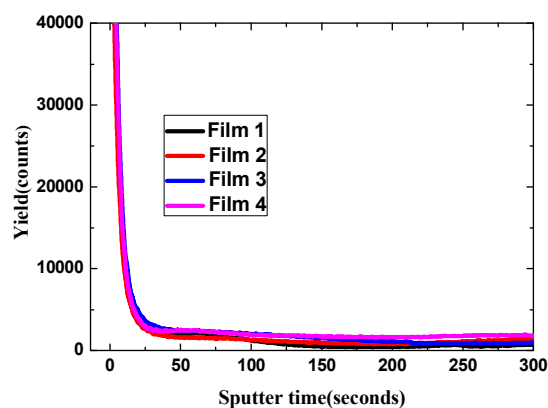


Fig. 5. Depth profile of film 1, film 2, film 3 and film 4 measured by TOF-SIMS: F⁻.

Table 3. The yield of F⁻ on the different sputter time of the films

sputter time[seconds]	Film 1	Film 2	Film 3	Film 4
5	4.25×10^5	3.25×10^5	3.80×10^5	3.74×10^5
150	1.02×10^3	1.93×10^3	2.95×10^3	3.45×10^3
300	1.42×10^3	2.88×10^3	1.92×10^3	3.54×10^3

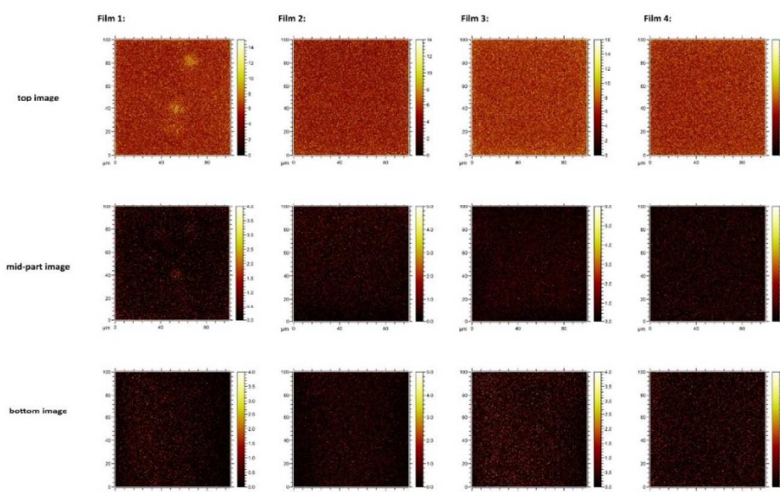


Fig. 6. TOF-SIMS images of F⁻ showing the blend compositions at various position with an analyzed area of $100 \times 100 \mu\text{m}$.

Fig. 7 reveals the effect of the additive treatment on the photocurrent density (J_{ph}). The value of J_{ph} is calculated by the equation $J_{\text{ph}} = J_{\text{L}} - J_{\text{D}}$, where J_{L} and J_{D} are the current densities under illumination and in the dark, respectively. **Fig. 7** is the plot of

J_{ph} with respect to the effective voltage $V_{eff}=V_o-V$, where V_o is the compensation voltage at which J_{ph} equals zero and V is the applied voltage. The saturation photocurrent density (J_{sat}) is only limited by total amount of absorbed incident photons if we assume that all the photogenerated excitons are dissociated into free charge carriers and collected by electrodes at a high V_{eff} .^{31, 32} J_{sat} is 8.0 mA/cm² for device 1, 12.3 mA/cm² for device 2, 13.2 mA/cm² for device 3, and 15.2 mA/cm² for device 4, respectively. The increased J_{sat} should be attributed to effective charge carrier transport and collection for the PSCs with additive treatment.³³ To gain more insight into the influence of the additives on exciton generation, we measured the maximum exciton generation rate (G_{max}) of our PSC devices. G_{max} could then be calculated using $J_{ph} = eG_{max}L$, where L is the thickness of active layer. From Figure 5, the values of G_{max} for the devices are $5.62 \times 10^{27} \text{ m}^{-3} \text{ s}^{-1}$, $9.26 \times 10^{27} \text{ m}^{-3} \text{ s}^{-1}$, $1.16 \times 10^{28} \text{ m}^{-3} \text{ s}^{-1}$ and $1.61 \times 10^{28} \text{ m}^{-3} \text{ s}^{-1}$ respectively. G_{max} slightly increased after the addition of additives, suggesting increased light absorption in device with additives;³². This matches well with increased absorption from the absorption spectra.

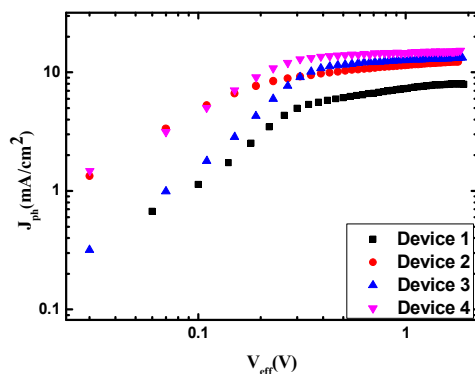


Fig.7. Photocurrent density versus effective voltage ($J_{ph}-V_{eff}$) characteristics without or with 3 v/v % DIO and 3 v/v % 1,8-Dibromooctane.

In order to further investigate solvent additive effect on the charge carrier transport, the hole-only devices were fabricated based on pristine PTB7 films and blend PTB7:PC₇₁BM films with/without additives, respectively. High-work-function material gold (Au) is used as the cathode to block the back injection of electrons. The dark J–V curves of the hole-only devices with the configuration of ITO/PEDOT:PSS/

PTB7/Au and ITO/PEDOT:PSS/ PTB7:PC₇₁BM /Au were measured and shown in **Fig.8**. The hole transport through the polymer film is limited due to the accumulation of space charge when a sufficient voltage is applied to this hole-only device. The space charge limited current(SCLC) is described by the equation^{34, 35}

$$J = \frac{9}{8} \epsilon \mu \frac{V^2}{d^3} = \frac{9}{8} \epsilon_0 \epsilon_r \mu \frac{V^2}{d^3} \quad (2)$$

where ϵ_0 is the permittivity of free space, ϵ_r is the dielectric constant of the blend material, μ is the hole mobility, V is the voltage drop across the device and d is the active layer thickness. The parameter ϵ_r was assumed to be 3, which is a typical value for conjugated polymers. The hole will be collected by the ITO electrode, which is very similar with hole transport process in the PSCs. The J–V characteristics of neat PTB7 and PTB7:PC₇₁BM with/without co-additive of 3 v/v % DIO and 3 v/v% 1,8-Dibromooctane fully agree with the SCLC model. According to the J–V curves, the hole current density of hole-only devices with 3 v/v % 1,8-Dibromooctane is larger than that of hole-only devices without any additive; and the hole current density of hole-only devices with 3 v/v % DIO is larger than that of hole-only devices with 3 v/v % 1,8-Dibromooctane. Moreover, the hole current density of hole-only devices with co-additive of both 3 v/v % DIO and 3 v/v % 1,8-Dibromooctane is larger than that of hole-only devices with only 3 v/v % DIO. This means that hole carrier transport in hole-only devices with 3 v/v % DIO and/or 3 v/v % 1,8-Dibromooctane has been improved compared with that of hole-only devices without any additive. The enhanced current density of the hole only device with 3 v/v % DIO and/or 3 v/v % 1,8-Dibromooctane further demonstrates that the improved hole carrier transport could be the main reason for the increased J_{sc} of PSCs.^{35, 36}

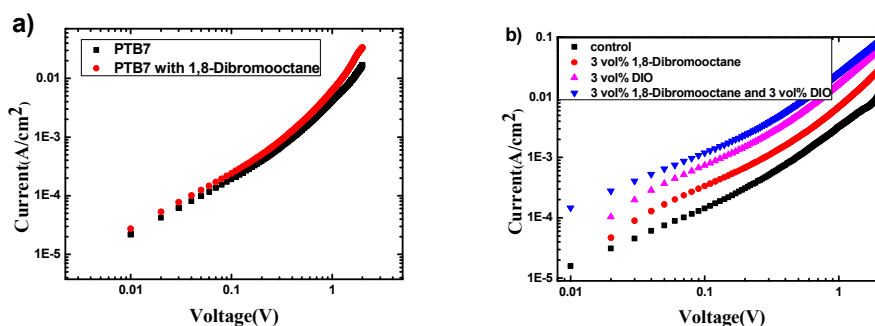


Fig.8.J–V characteristic curves of hole-only devices with/without 3 v/v % DIO and/or 3 v/v % 1,8-Dibromooctane.

4. Conclusion

A series of PSCs with PTB7:PC₇₁BM as the active layer were fabricated to investigate the solvent additive effect on the performance of PSCs. DIO and 1,8-Dibromooctane were used as the solvent additives. The experimental result of photovoltaic performance reveals an enhancement of J_{sc} from 7.22 to 14.35 mA/cm² and FF from 50.0% to 65.4% by adding DIO and 1,8-Dibromooctane as co-additive. As the result, the PCEs of PSCs were improved from 2.74% to 6.76%, with 146.7% improvement compared with PSCs based on PTB7:PC₇₁BM without additives. The positive effect of DIO and 1,8-Dibromooctane additives on the performance of PSCs should be attributed to the absorption enhancement and the increased charge carrier transport and collection.

Acknowledgement

This work was supported by the Fundamental Research Funds for the National Natural Science Foundation of China (No. 51272022), the National High Technology Research and Development Program of China (863 Program) (No. 2013AA032205), the Research Fund for the Doctoral Program of Higher Education (Nos. 20120009130005 and 20130009130001), and the Fundamental Research Funds for the Central Universities (No. 2012JBZ001)

References and Notes

1. L. Dou, J. You, J. Yang, C.-C. Chen, Y. He, S. Murase, T. Moriarty, K. Emery, G. Li and Y. Yang, *Nature Photonics*, 2012, 6, 180-185.
2. R. Meier, C. Birkenstock, C. M. Palumbiny and P. Müller-Buschbaum, *Physical Chemistry Chemical Physics*, 2012, 14, 15088-15098.
3. J. Kong, J. Lee, G. Kim, H. Kang, Y. Choi and K. Lee, *Physical Chemistry Chemical Physics*, 2012, 14, 10547-10555.
4. S. H. Liao, H. J. Jhuo, Y. S. Cheng and S. A. Chen, *Advanced Materials*, 2013, 25, 4766-4771.
5. Z. He, C. Zhong, X. Huang, W. Y. Wong, H. Wu, L. Chen, S. Su and Y. Cao, *Advanced Materials*, 2011, 23, 4636-4643.
6. H. Zhou, Q. Chen, G. Li, S. Luo, T.-b. Song, H.-S. Duan, Z. Hong, J. You, Y. Liu and Y. Yang, *Science*, 2014, 345, 542-546.

7. M. A. Green, *Progress in Photovoltaics: Research and Applications*, 2009, 17, 183-189.
8. Z. Liu, H. Ju and E.-C. Lee, *Applied Physics Letters*, 2013, 103, 133308.
9. Y. Liang, Z. Xu, J. Xia, S. T. Tsai, Y. Wu, G. Li, C. Ray and L. Yu, *Advanced Materials*, 2010, 22, E135-E138.
10. F. Zhang, K. G. Jespersen, C. Bjoerstroem, M. Svensson, M. R. Andersson, V. Sundström, K. Magnusson, E. Moons, A. Yartsev and O. Inganäs, *Advanced Functional Materials*, 2006, 16, 667-674.
11. J. Jo, S. S. Kim, S. I. Na, B. K. Yu and D. Y. Kim, *Advanced Functional Materials*, 2009, 19, 866-874.
12. J. K. Lee, W. L. Ma, C. J. Brabec, J. Yuen, J. S. Moon, J. Y. Kim, K. Lee, G. C. Bazan and A. J. Heeger, *Journal of the American Chemical Society*, 2008, 130, 3619-3623.
13. R. A. Janssen and J. Nelson, *Advanced materials*, 2013, 25, 1847-1858.
14. K. G. Lim, H. B. Kim, J. Jeong, H. Kim, J. Y. Kim and T. W. Lee, *Advanced Materials*, 2014, 26, 6461-6466.
15. K. G. Lim, M. R. Choi, J. H. Kim, D. H. Kim, G. H. Jung, Y. Park, J. L. Lee and T. W. Lee, *ChemSusChem*, 2014, 7, 1125-1132.
16. M. R. Choi, S. H. Woo, T. H. Han, K. G. Lim, S. Y. Min, W. M. Yun, O. K. Kwon, C. E. Park, K. D. Kim and H. K. Shin, *ChemSusChem*, 2011, 4, 363-368.
17. T. H. Han, M. R. Choi, S. H. Woo, S. Y. Min, C. L. Lee and T. W. Lee, *Advanced Materials*, 2012, 24, 1487-1493.
18. S. J. Lou, J. M. Szarko, T. Xu, L. Yu, T. J. Marks and L. X. Chen, *Journal of the American Chemical Society*, 2011, 133, 20661-20663.
19. S. Ochiai, S. Imamura, S. Kannappan, K. Palanisamy and P.-K. Shin, *Current Applied Physics*, 2013, 13, S58-S63.
20. X. Hu, M. Wang, F. Huang, X. Gong and Y. Cao, *Synthetic metals*, 2013, 164, 1-5.
21. S. Guo, J. Ning, V. Körstgens, Y. Yao, E. M. Herzig, S. V. Roth and P. Müller - Buschbaum, *Advanced Energy Materials*, 2014.
22. B. A. Collins, Z. Li, J. R. Tumbleston, E. Gann, C. R. McNeill and H. Ade, *Advanced Energy Materials*, 2013, 3, 65-74.
23. X. Fan, G. Fang, P. Qin, F. Cheng and X. Zhao, *Applied Physics A*, 2011, 105, 1003-1009.
24. H. Tang, G. Lu, L. Li, J. Li, Y. Wang and X. Yang, *Journal of Materials Chemistry*, 2010, 20, 683-688.
25. D. T. Duong, B. Walker, J. Lin, C. Kim, J. Love, B. Purushothaman, J. E. Anthony and T. Q. Nguyen, *Journal of Polymer Science Part B: Polymer Physics*, 2012, 50, 1405-1413.
26. W. A. Hammed, R. Yahya, A. u. L. Bola and H. N. M. E. Mahmud, *Energies*, 2013, 6, 5847-5868.
27. P. Kumar, S. Kannappan, S. Ochiai and P.-K. Shin, *Journal of the Korean Physical Society*, 2013, 62, 1169-1175.
28. J. M. Szarko, B. S. Rolczynski, S. J. Lou, T. Xu, J. Strzalka, T. J. Marks, L. Yu and L. X. Chen, *Advanced Functional Materials*, 2014, 24, 10-26.
29. B.-Y. Yu, W.-C. Lin, W.-B. Wang, S.-i. Iida, S.-Z. Chen, C.-Y. Liu, C.-H. Kuo, S.-H. Lee, W.-L. Kao and G.-J. Yen, *Acs Nano*, 2010, 4, 833-840.
30. J. P. Thomas, L. Zhao, M. Abd-Ellah, N. F. Heinig and K. T. Leung, *Analytical chemistry*, 2013, 85, 6840-6845.

31. C. Shuttle, R. Hamilton, B. O'Regan, J. a. Nelson and J. Durrant, *Proceedings of the National Academy of Sciences*, 2010, 107, 16448-16452.
32. L. Lu, T. Xu, W. Chen, J. M. Lee, Z. Luo, I. H. Jung, H. I. Park, S. O. Kim and L. Yu, *Nano letters*, 2013, 13, 2365-2369.
33. F. Zhang, Z. Zhuo, J. Zhang, X. Wang, X. Xu, Z. Wang, Y. Xin, J. Wang, J. Wang and W. Tang, *Solar Energy Materials and Solar Cells*, 2012, 97, 71-77.
34. G. Malliaras, J. Salem, P. Brock and C. Scott, *Physical Review B*, 1998, 58, R13411.
35. Z. Wang, F. Zhang, L. Li, Q. An, J. Wang and J. Zhang, *Applied Surface Science*, 2014, 305, 221-226.
36. J. Wang, F. Zhang, L. Li, Q. An, J. Zhang, W. Tang and F. Teng, *Solar Energy Materials and Solar Cells*, 2014, 130, 15-19.